

Hidden and antiferromagnetic order as a rank-5 superspin in URu₂Si₂

Jeffrey G. Rau¹ and Hae-Young Kee^{1,2,*}

¹*Department of Physics, University of Toronto, Toronto, Ontario M5S 1A7, Canada*

²*Canadian Institute for Advanced Research/Quantum Materials Program, Toronto, Ontario MSG 1Z8, Canada*

(Received 12 March 2012; published 13 June 2012)

We propose a candidate for the hidden order in URu₂Si₂: a rank-5 E type spin-density wave between uranium $5f$ crystal-field doublets $\Gamma_7^{(1)}$ and $\Gamma_7^{(2)}$, breaking time-reversal and lattice tetragonal symmetry in a manner consistent with recent torque measurements [Okazaki *et al.*, *Science* **331**, 439 (2011)]. We argue that coupling of this order parameter to magnetic probes can be hidden by crystal-field effects, while still having significant effects on transport, thermodynamics, and magnetic susceptibilities. In a simple tight-binding model for the heavy quasiparticles, we show the connection between the hidden order and antiferromagnetic phases arises since they form different components of this single rank-5 pseudospin vector. Using a phenomenological theory, we show that the experimental pressure-temperature phase diagram can be qualitatively reproduced by tuning terms which break pseudospin rotational symmetry. As a test of our proposal, we predict the presence of small magnetic moments in the basal plane oriented in the [110] direction ordered at the wave vector (0,0,1).

DOI: 10.1103/PhysRevB.85.245112

PACS number(s): 71.27.+a, 75.30.Mb

I. INTRODUCTION

The nature of the low-temperature ordered phase found in the heavy fermion compound URu₂Si₂ has defied explanation for over 25 years. While the transition into this hidden order (HO) phase appears quite conventional based on the effects on thermodynamic,^{1,2} magnetic,²⁻⁴ and transport phenomena,^{2,5,6} the order parameter itself remains elusive. This stands in contrast to the significant entropy release² across the transition, indicating a strong ordering, inconsistent with the weak antiferromagnetic moments that perplexed early studies. Heroic efforts have brought the full complement of experimental techniques to bear upon this problem, from local probes such as μ SR,⁷ NMR^{8,9} and NQR,¹⁰ surface probes,¹¹⁻¹³ scattering studies using elastic and inelastic neutrons^{3,14,15} and resonant x rays,^{16,17} as well as explorations of the material through pressure, both hydrostatic^{15,18,19} and uniaxial²⁰ and high magnetic fields.²¹ Key facets of the problem illuminated by these studies include a pressure induced antiferromagnetic phase (AF) and a superconducting phase that arises out of the HO phase. Similarities between the HO and AF phases, such as their Fermi surfaces,^{22,23} suggest a common underlying mechanism. While great progress has been made, the central mystery of the identity of the HO still remains.

Recently, an important clue to the nature of the HO has been seen in magnetic torque experiments.²⁴ Through a measurement of the off-diagonal magnetic susceptibility on small samples, it was found that the HO phase breaks the rotational symmetry of the crystal spontaneously in the [110] direction. Lack of detectable lattice distortions^{25,26} suggests that this symmetry breaking is purely an electronic phenomenon. This is inconsistent with many earlier theoretical proposals for the HO (see Ref. 27 for a review) and thus has attracted a great deal of interest. New proposals to explain these observations include, among others, spin-nematic states,²⁸ dynamical symmetry breaking,^{29,30} staggered spin-orbit coupling order,³¹ and hastatic order.³²

In this paper, we propose a candidate for the hidden order in URu₂Si₂ as a rank-5 E type spin-density wave between $5f$ crystal-field doublets $\Gamma_7^{(1)}$ and $\Gamma_7^{(2)}$. This breaks both time-

reversal and the lattice point-group symmetry D_{4h} in a manner consistent with the torque result. We argue that the expected coupling of this order parameter to magnetic probes, such as neutrons, can be effectively hidden by crystal-field effects in the magnetic moment, while still contributing to second-order correlations such as susceptibilities. This would manifest as a small moment in the basal plane oriented along the [110] direction ordered at wave vector (0,0,1). In a simple tight-binding model for the itinerant heavy quasiparticles, we show that the close relation between the HO and AF phases arises due to an approximate degeneracy between the E type (x and y components) and A_2 type (z component) of the rank-5 pseudospin vector,³³

$$\vec{\phi} = \left\langle \frac{1}{N} \sum_i e^{i\vec{Q}\cdot\vec{r}_i} \left(\frac{\vec{S}_{12}(i) + \vec{S}_{21}(i)}{\sqrt{2}} \right) \right\rangle, \quad (1)$$

where $\vec{Q} = 2\pi/c\hat{z} \equiv (0,0,1)$ and we have defined generalized spin operators $\vec{S}_{\alpha\beta} = \frac{1}{2} f_{\alpha}^{\dagger} \vec{\sigma} f_{\beta}$ where $\alpha, \beta = 1, 2$ indicate the $\Gamma^{(7)}$ doublet. These doublets are related to the $5f$ J_z eigenstates as $f_{1\pm} = \cos\theta f_{\pm 5/2} + \sin\theta f_{\mp 3/2}$ and $f_{2\pm} = -\sin\theta f_{\pm 5/2} + \cos\theta f_{\mp 3/2}$ where θ is determined by the relative crystal-field strengths.³⁴ The similarity of the Fermi surfaces arises as the breaking of the pseudospin symmetry is inoperative in the k_x - k_y plane, leading to similar cross sections and thus oscillations. Using a phenomenological theory, we show that the experimental phase diagram as a function of pressure and temperature can be qualitatively reproduced by tuning either the hopping which breaks pseudospin rotational symmetry or the effective coupling constants. As a consequence of this pseudospin symmetry breaking, the Goldstone mode connecting the HO and AF becomes gapped, leading to a resonance a finite frequency in the magnetic response. Specific heat and magnetic susceptibilities are also presented, and experimental means to test our proposal are discussed.

II. MODEL

The heavy-fermion physics of URu₂Si₂ is signalled by a peak in the magnetic susceptibility² indicating a coherence

temperature ~ 60 K, well above the hidden order transition temperature T_O . It is reasonable to assume that near the HO phase the relevant physics is encompassed by that of a (heavy) Fermi liquid. Recent work^{12,28–30} supports this, suggesting itinerant character for the U $5f$ electrons, with coherent U dominant quasiparticles near the Fermi surface, can account for many of the properties of the paramagnetic state.

Motivated by this, we consider single-particle $5f$ states in a crystal field of D_{4h} symmetry, using the notation of Ref. 34 for the irreducible representations of D_{4h} . The strong atomic spin-orbit coupling splits the $5f$ levels into a low-lying $j = 5/2$ sextet and high-lying $j = 7/2$ octet. Since the $j = 7/2$ states lie significantly higher in energy than the $j = 5/2$, we keep only the latter in our discussion. Under the potential of the crystal lattice this sextet splits into three Kramers doublets, as $\Gamma_{5/2} = 2\Gamma_7 \oplus \Gamma_6$, explicitly

$$\begin{aligned} f_{1\pm} &= \cos\theta f_{\pm 5/2} + \sin\theta f_{\mp 3/2}, \\ f_{2\pm} &= -\sin\theta f_{\pm 5/2} + \cos\theta f_{\mp 3/2}, \\ f_{3\pm} &= f_{\pm 1/2}. \end{aligned}$$

We consider a tight-binding model for URu₂Si₂ using states with $\Gamma_7^{(1)}$, $\Gamma_7^{(2)}$, and Γ_6 character, including contributions from nearest- and next-nearest-neighbor hoppings. The Γ_6 bands are involved in producing the incommensurate inelastic neutron peak,³ at a nesting wave vector connecting Γ_7 and Γ_6 , through the gapping of Γ_7 Fermi surface in the ordered phases. For the sake of simplicity we focus only on Fermi surfaces of Γ_7 character as they form the superspin of the current study. If we include hoppings along the body diagonals, as well as along the in-plane axes and diagonals, symmetry restrict us to a Hamiltonian of the form

$$\begin{aligned} H_0 &= \sum_{k\sigma} (A_{1k} f_{1\sigma,k}^\dagger f_{1\sigma,k} + A_{2k} f_{2\sigma,k}^\dagger f_{2\sigma,k}) \\ &+ \sum_k (C_k f_{1+,k}^\dagger f_{2+,k} + C_k^* f_{1-,k}^\dagger f_{2-,k} + \text{H.c.}) \\ &+ \sum_k (D_k f_{1+,k}^\dagger f_{2-,k} - D_k^* f_{1-,k}^\dagger f_{2+,k} + \text{H.c.}), \quad (2) \end{aligned}$$

where $f_{\alpha\sigma}^\dagger$, with $\alpha = 1, 2$, $\sigma = \pm$ creates a state in the $\Gamma_7^{(\alpha)}$ doublet with pseudospin σ . To obtain a Fermi surface that matches our criteria above, we find it possible to take $C_k = 0$. The remaining dispersion functions take the form

$$\begin{aligned} A_{\alpha k} &= 8t_a \cos\left(\frac{ak_x}{2}\right) \cos\left(\frac{ak_y}{2}\right) \cos\left(\frac{ak_z}{2}\right) \\ &+ 2t'_a [\cos(ak_x) + \cos(ak_y)] \\ &+ 4t''_a \cos(ak_x) \cos(ak_y) - \mu + \text{sgn}(\alpha) \frac{\Delta_{12}}{2}, \\ D_k &= 4t_{12} \left[\sin\left(\frac{a(k_x + k_y)}{2}\right) - i \sin\left(\frac{a(k_x - k_y)}{2}\right) \right] \\ &\times \sin\left(\frac{ck_z}{2}\right), \end{aligned}$$

where Δ_{12} is the effective crystal-field splitting between $\Gamma_7^{(1)}$ and $\Gamma_7^{(2)}$ levels, $\text{sgn}(\alpha) = \pm 1$ for $\alpha = 1, 2$, and c and a are the lattice constants. Physically, t_a represents hopping along the $a(\hat{x} + \hat{y}) + \frac{c}{2}\hat{z}$ and equivalent directions, t'_a along $a\hat{x}$ and

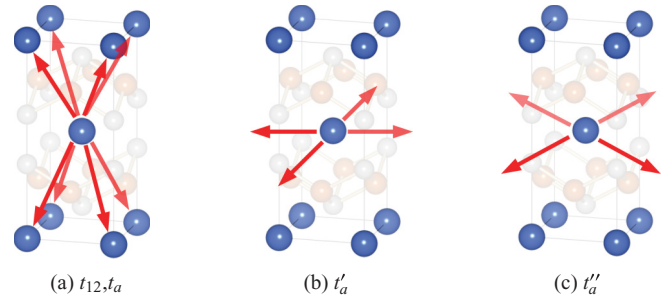


FIG. 1. (Color online) Graphical representation of the relevant hopping amplitudes along the (a) body diagonal, (b) in-plane axes, and (c) in-plane diagonals shown in the unit cell of URu₂Si₂.

$a\hat{y}$ and t''_a along $a(\hat{x} + \hat{y})$ and equivalent directions, as shown in Fig. 1. In the following we fix hoppings $t_1 = t_2 = -0.3$, $t'_1 = -0.87$, $t'_2 = 0.0$, $t''_1 = 0.375$, $t''_2 = 0.25$ with chemical potential $\mu = -0.5$ and crystal-field splitting $\Delta_{12} = 3.5$. For concreteness we take $|t_{12}| = 0.7$ in the Fermi-surface plots, but will allow it to vary when discussing phenomenological models. We note that Fermi surface does not depend strongly on the choice of t_{12} . Geometrically, one expects this t_{12} hopping to be related to hybridization with the Ru d orbitals. As we have neglected several bands from our description, we treat the remainder of the system as a charge reservoir, keeping the chemical potential fixed and allowing the density to vary. We note that for $t_{12} = 0$ this tight-binding model has global SU(2) pseudospin-rotation symmetry within each doublet. For finite t_{12} this is broken to a single extra U(1) symmetry between the $\Gamma_7^{(1)}$ and $\Gamma_7^{(2)}$ doublets, transforming $f_{1\sigma} \rightarrow e^{i\sigma\psi} f_{1\sigma}$ and $f_{2\sigma} \rightarrow e^{-i\sigma\psi} f_{2\sigma}$.

Using the above hopping parameters, the Fermi surface shown in Fig. 2 is obtained. These parameters have been chosen to respect the following experimental and theoretical results. From Hall and magnetoresistivity measurements, one expects closed electron and hole Fermi surfaces of nearly equal size. *Ab initio* calculations suggest that these electron and hole pockets are composed mainly of $\Gamma_7^{(1)}$ and $\Gamma_7^{(2)}$. Furthermore, the similarity of the Fermi surfaces in the HO and AF states and nesting between the electron and hole Fermi surfaces at the AF ordering vector \vec{Q} strongly suggests that the HO and AF orderings occur at the same wave vector. Under this

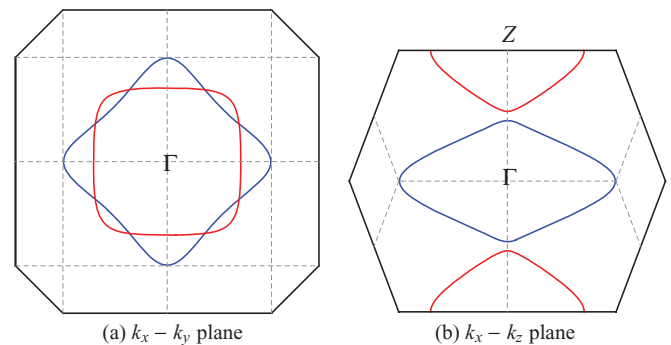


FIG. 2. (Color online) (a) View of the Fermi surfaces in the k_x - k_y plane. The holelike Fermi surface (red) is centered about $k_z = 2\pi/c$ while the electronlike Fermi surface (blue) is centered about Γ . (b) View of the Fermi surfaces in the k_x - k_z plane.

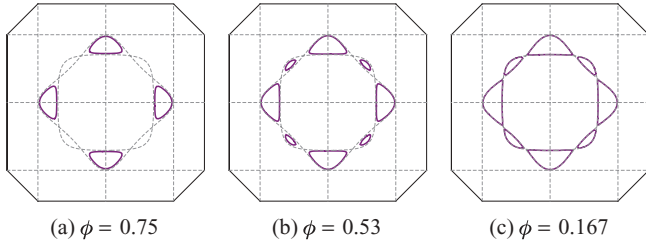


FIG. 3. (Color online) Fermi surface after imposition of finite $\phi = |\phi|$ in the $k_z = 0$ plane for several values of ϕ (in the unfolded Brillouin zone).

assumption we then need the nesting to be imperfect to match the small pockets observed in oscillation measurements.^{18,22} This is implemented in a fashion consistent with *ab initio* results, with the electron pocket near Γ being elongated in the [100] and [010] directions and the hole pocket at Z being elongated in the [110] and [1 $\bar{1}$ 0] directions. After folding along \vec{Q} one then has four small pockets along [100] and [010] as shown in Fig. 3.

III. ORDER PARAMETER

The key signals found in the torque measurements are $\chi_{xy} \neq 0$ and $\chi_{xx} = \chi_{yy}$ within the HO phase. Landau-Ginzburg arguments³⁴ show that an order parameter consistent with these facts and their temperature dependence should transform as the two-dimensional E irreducible representation³⁵ of the D_{4h} point group, with periodicity at the wave vector \vec{Q} . The details of the torque oscillations single out a set of symmetry related directions in this two-dimensional space, namely the four orientations $(\pm 1, \pm 1)$, so we will denote this type of order parameter as $E(1,1)$. In the picture outlined above, where the relevant degrees of freedom are the two Γ_7 bands, there are only two local E -type order parameters that mix f_1 and f_2 , taking advantage of the nesting at \vec{Q} . These are the x and y components of the vectors $i(\vec{S}_{12} - \vec{S}_{21})$ or $\vec{S}_{12} + \vec{S}_{21}$.

The first E -type order parameter is inconsistent with resonant x-ray scattering results¹⁷ as it carries an electric quadrupole moment. The second breaks time reversal and, as the in-plane components of the magnetic-moment operator also transform as E , an induced magnetic moment is expected generically. This can be seen explicitly by restricting to the Γ_7 doublets and constructing the moment operator $\vec{\mu} = \vec{L} + 2\vec{S}$ at each site in the Γ_7 basis,

$$\begin{aligned}\mu_x &= \frac{6\sqrt{5}}{7} [\sin(2\theta)(S_{11}^x - S_{22}^x) + \cos(2\theta)(S_{12}^x + S_{21}^x)], \\ \mu_y &= \frac{6\sqrt{5}}{7} [\sin(2\theta)(S_{11}^y - S_{22}^y) + \cos(2\theta)(S_{12}^y + S_{21}^y)], \\ \mu_z &= \frac{24}{7} [\cos(2\theta)(S_{11}^z - S_{22}^z) - \sin(2\theta)(S_{12}^z + S_{21}^z)] \\ &\quad + \frac{6}{7} [S_{11}^z + S_{22}^z].\end{aligned}\quad (3)$$

For $\theta = \frac{\pi}{4} + \delta$ with δ small, the terms proportional to $\vec{S}_{12} + \vec{S}_{21}$ in the x and y components are $O(\delta)$, while the z component remains $O(1)$. One has the scenario that for small δ the magnetic coupling to this type of E order parameter is

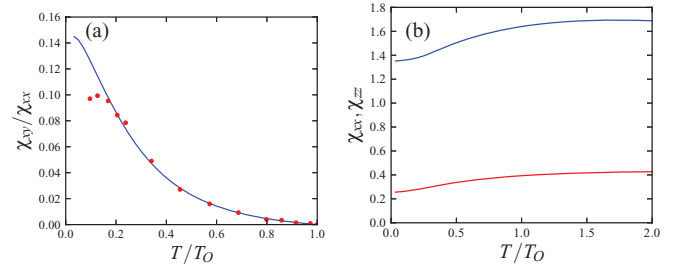


FIG. 4. (Color online) (a) The off-diagonal magnetic susceptibility χ_{xy} in $E(1,1)$ at a function of temperature. One can obtain a strong resemblance to the measured susceptibility in Ref. 24, shown in red, by fitting the overall amplitude of χ_{xy}/χ_{xx} and the position of T_0 . (b) The uniform magnetic susceptibility in $E(1,1)$ phase as a function of temperature. Both $\chi_{xx} = \chi_{yy}$ (red) and χ_{zz} (blue) are shown.

significantly reduced.³⁶ For example, the neutron scattering cross section is $O(\delta^2)$. For these reasons we take the x and y components of Eq. (1) as the HO with the z component as the AF.³⁷ Note that even though the expectation is suppressed, the presence of other terms, $\sim \sin(2\theta)$, in the moment operator allows terms of $O(1)$ to present in the in-plane susceptibilities. The bare susceptibilities in the $E(1,1)$ phase are shown in Fig. 4. The temperature dependence of the χ_{xy} signal is strikingly similar to that found in the torque experiments. Deviations at the lowest temperatures are likely due to effects from the superconducting phase.

IV. PHENOMENOLOGICAL THEORY

Due to the approximate nesting of the Fermi surfaces, the similarity to the AF state, and the implications of the Landau-Ginzburg analysis of the torque experiments,³⁴ we consider only ordering at wave vector \vec{Q} . To explore this scenario, consider the phenomenological model, where the tight-binding model is supplemented by the coupling terms

$$\begin{aligned}H_\phi &= -\frac{\vec{\phi}}{\sqrt{2}} \cdot \sum_i e^{i\vec{Q}\cdot\vec{r}_i} (\vec{S}_{12}(i) + \vec{S}_{21}(i)), \\ &= -\frac{\vec{\phi}}{2\sqrt{2}} \cdot \sum_k (f_{1,k}^\dagger \vec{\sigma} f_{2,k+\vec{Q}} + f_{2,k}^\dagger \vec{\sigma} f_{1,k+\vec{Q}} + \text{H.c.}),\end{aligned}\quad (4)$$

where the momentum sum runs over the reduced Brillouin zone, folded along \vec{Q} , as well as the quadratic terms,

$$N \left(\frac{1}{2g_{xy}} (\phi_x^2 + \phi_y^2) + \frac{1}{2g_z} \phi_z^2 \right), \quad (5)$$

where we have introduced the couplings g_{xy} and g_z . The $E(1,1)$ phase corresponds to $|\phi_x| = |\phi_y| \equiv \phi$ and $\phi_z = 0$. The phase where $\phi_x = \phi_y = 0$ and $\phi_z \neq 0$ is magnetic, without any suppression factors of δ in the magnetic coupling, and does not break the C_4 symmetry present in the point group. We identify this with the pressure induced AF phase.

Explicitly, we first write the kinetic part of the Hamiltonian as

$$H_0 = \sum_k \Psi_k^\dagger \begin{pmatrix} A_{1k} & 0 & 0 & D_k \\ 0 & A_{1k} & -D_k^* & 0 \\ 0 & -D_k & A_{2k} & 0 \\ D_k^* & 0 & 0 & A_{2k} \end{pmatrix} \Psi_k \quad (6)$$

$$\equiv \sum_k \Psi_k^\dagger \begin{pmatrix} A_{1k} & \gamma_k \\ \gamma_k^\dagger & A_{2k} \end{pmatrix} \Psi_k, \quad (7)$$

where $\Psi_k^\dagger = (f_{1+,k}^\dagger, f_{1-,k}^\dagger, f_{2+,k}^\dagger, f_{2-,k}^\dagger)$ and $\gamma_k = i\sigma_y \text{Re}D_k + i\sigma_x \text{Im}D_k$. Then the phenomenological Hamiltonian is given by

$$H = \sum_k \begin{pmatrix} \Psi_k \\ \Psi_{k+Q} \end{pmatrix}^\dagger \begin{pmatrix} A_{1k} & \gamma_k & 0 & -\frac{\vec{\phi} \cdot \vec{\sigma}}{2\sqrt{2}} \\ \gamma_k^\dagger & A_{2k} & -\frac{\vec{\phi} \cdot \vec{\sigma}}{2\sqrt{2}} & 0 \\ 0 & -\frac{\vec{\phi} \cdot \vec{\sigma}}{2\sqrt{2}} & A_{1k+Q} & \gamma_{k+Q} \\ -\frac{\vec{\phi} \cdot \vec{\sigma}}{2\sqrt{2}} & 0 & \gamma_{k+Q}^\dagger & A_{2k+Q} \end{pmatrix} \begin{pmatrix} \Psi_k \\ \Psi_{k+Q} \end{pmatrix}, \quad (8)$$

where the momentum sum now runs over the reduced Brillouin zone. In this general form one cannot access the spectrum analytically of Eq. (8), but since for $k_z = 0$ the off-diagonal term D_k is zero, one can find the spectrum in this plane, yielding branches E_k^\pm and E_{k+Q}^\pm where

$$E_k^\pm = \frac{A_{1k} + A_{2,k+Q}}{2} \pm \sqrt{\left(\frac{A_{1k} - A_{2,k+Q}}{2}\right)^2 + \left|\frac{\vec{\phi}}{2\sqrt{2}}\right|^2}.$$

This implies that the Fermi surfaces have the same cross sections at $k_z = 0$, independent of the orientation of $\vec{\phi}$. This naturally explains the similarity in the oscillation measurements^{18,22} in the HO and AF phases and the remaining small pockets. The Fermi surface for various values of $|\vec{\phi}|$ is shown in Fig. 3. As the ordering is strengthened, the remaining Fermi surfaces form four small pockets along the x and y axes. This removal of large sections of the Fermi surface within the HO phase is qualitatively consistent with implications from transport and specific heat measurements.² The destruction of the pockets along the diagonal directions occurs due to more robust nesting in planes along the intersection points of the electron and hole Fermi surfaces. A similar feature has been noted in recent *ab initio* Fermi surfaces.³⁰

A key signature of the HO phase is the inelastic neutron-scattering peak at \vec{Q} . To examine this the imaginary part of the bare susceptibility at the ordering vector \vec{Q} , $\text{Im}\chi_{zz}(\vec{Q}, \omega)$ is computed and shown in Fig. 5(a). There is a clear gap below a peak at finite frequency, reminiscent of the neutron results. The specific heat shown in Fig. 5(b) also shows a clear jump at T_O as expected, but the calculated value is too small to be realistically compared with the experimental results. The precise size of jump in the model depends on the strength of order parameter ϕ , tendency of nesting on the Fermi surface, interaction effects, and details of the some the other bands that have been left out of our model (for example from the gapping of the incommensurate modes).

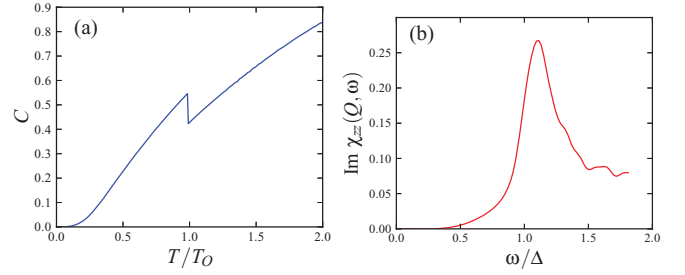


FIG. 5. (Color online) (a) The specific heat as a function of temperature. Note the jump at T_O . (b) The imaginary part of the susceptibility in the zz channel at \vec{Q} at $T = 0$. The frequency ω is scaled by the gap at perfect nesting $\Delta = |\vec{\phi}|/\sqrt{2}$.

To study the transition for the HO to AF phases we look at the mean-field phase diagram as a function of temperature, effective coupling constants g_{xy} and g_z , and t_{12} , the hopping which breaks pseudospin rotation symmetry. One can evaluate the free energy for this Hamiltonian numerically, including the quadratic parts of Eq. (5), and minimize to find the value of ϕ . As the locking of the pseudospin orientation to the spatial orientation is controlled by the t_{12} hopping, to obtain an $E(1, 1)$ phase over a $E(1, 0)$ or $E(0, 1)$ phase we choose the phase of t_{12} to be $\pi/4$. This is supported by Slater-Koster-type calculations of t_{12} , which also yield a phase of $\pi/4$. We find that for any finite value of t_{12} with equal couplings, $g_{xy} = g_z$, the AF state is favored. This allows for a scenario where $g_{xy} > g_z$ and t_{12} increases as pressure is raised from ambient, causing a transition from HO to AF as shown in Fig. 6(a). A more direct possibility is allowing g_z/g_{xy} to vary from $g_{xy} > g_z$ at ambient pressure to $g_z > g_{xy}$ at higher pressure, and fixing t_{12} , as shown in Fig. 6(b). In both these cases the HO to AF transition is first order, and the qualitative topology is similar to that seen as a function of pressure and temperature in URu_2Si_2 .

V. DISCUSSION

An important ingredient in this proposal is the fine-tuning of the crystal-field angle θ to be near enough to $\pi/4$ to have the basal plane moments avoid detection thus far. Depending on the magnitude of the deviation δ , the order parameter should be observable in polarized neutron scattering. This leads to a prediction of small moment in the basal plane in the HO phase, oriented along $[110]$. So far, neutron scattering has

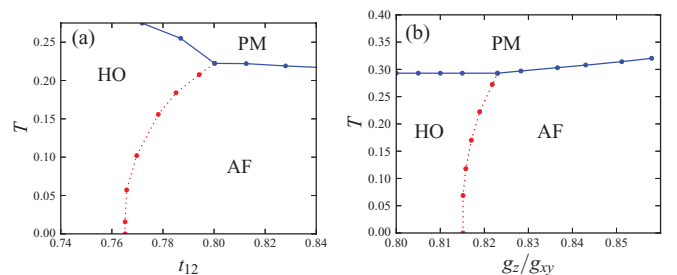


FIG. 6. (Color online) (a) Mean-field phase diagram as a function of the hopping parameter t_{12} , which breaks the HO-AF degeneracy, at $g_z/g_{xy} = 0.8$. (b) Phase diagram as a function of the coupling constant ratio g_z/g_{xy} where $t_{12} = 0.7$ and $g_{xy} = 5.0$.

been focused on scattering at wave vector $(1,0,0)$, favorable to detecting ordering oriented along the z axis. Furthermore, when (unpolarized) scattering is done at wave vector $(1,0,0)$ the small moment from the HO would be lost in the signal from the parasitic AF moment. To avoid a signal from the parasitic moment present in the HO phase, while still detecting a small moment along $[110]$, we suggest a careful neutron scattering analysis with wave vector $(0,0,1)$ (parallel to \vec{Q}) since the z component moment would not contribute due to the geometric factor in the scattering cross section. In particular, when neutron is polarized parallel to \vec{Q} , all magnetic scattering is spin-flip and should come from the basal plane moment. Polarized scattering along $(1,0,0)$ should also be effective at uncovering the moment, so long as the sensitivity is sufficiently high. While the quantitative determination of the angle θ , and thus expected moment size to be seen in experiment, is beyond the scope of the current study, recent LDA + U calculations³⁸ suggest that such fine-tuning could be realized in URu₂Si₂. Effects of high magnetic fields could also lead to testable implications of this model. One expects that at large enough fields this will destroy the HO due to breaking of nesting between the $\Gamma_7^{(1)}$ and $\Gamma_7^{(2)}$ orbitals. The complex structure of the magnetic moment operator in Eq. (3) could lead to nontrivial Fermi-surface splittings, perhaps leading the way to another type of ordering. The relation of this to the phases²¹ which appear in the vicinity of ~ 37 T warrants a detailed study, which we leave to future work.

In summary, we have presented a simple effective tight-binding model for the relevant bands in URu₂Si₂. Motivated from this model, we propose that the HO is realized as a rank-5 interorbital spin-density wave oriented along the $[110]$ direction. This gives the correct breaking of tetragonal symmetry to account for the recent torque results.²⁴ A natural relation between the HO and AF phases is provided, connecting them through a pseudospin rotation as well as explaining the similarity of their Fermi surfaces. The Goldstone mode in the HO is gapped due to terms that break pseudospin rotational symmetry, manifesting as the finite frequency peak seen in inelastic neutron-scattering experiments. The pressure-temperature phase diagram is also understood through this symmetry breaking. While the size of the moment in the basal plane in the HO can be suppressed by fine-tuning of the crystal-field strengths, it should be detectable by polarized neutron scattering.

Note added. After completion of this work, we have been made aware of a first-principles LDA + U study³⁸ which has proposed a time-reversal breaking E -type order parameter as a strong candidate for the HO phase in URu₂Si₂. The smallness of the moment in this work lends support to our current proposal.

ACKNOWLEDGMENTS

We thank C. M. Puetter and J. A. Dror for useful discussions. This work was supported by the NSERC of Canada.

*hykee@physics.utoronto.ca

¹A. de Visser, F. E. Kayzel, A. A. Menovsky, J. J. M. Franse, J. van den Berg, and G. J. Nieuwenhuys, *Phys. Rev. B* **34**, 8168 (1986).

²T. T. M. Palstra, A. A. Menovsky, J. v. d. Berg, A. J. Dirkmaat, P. H. Kes, G. J. Nieuwenhuys, and J. A. Mydosh, *Phys. Rev. Lett.* **55**, 2727 (1985).

³C. Broholm, H. Lin, P. T. Matthews, T. E. Mason, W. J. L. Buyers, M. F. Collins, A. A. Menovsky, J. A. Mydosh, and J. K. Kjems, *Phys. Rev. B* **43**, 12809 (1991).

⁴A. P. Ramirez, P. Coleman, P. Chandra, E. Brück, A. A. Menovsky, Z. Fisk, and E. Bucher, *Phys. Rev. Lett.* **68**, 2680 (1992).

⁵J. Schoenes, C. Schönerberger, J. J. M. Franse, and A. A. Menovsky, *Phys. Rev. B* **35**, 5375 (1987).

⁶A. L. Dawson, W. R. Datars, J. D. Garrett, and F. S. Razavi, *J. Phys.: Condens. Matter* **1**, 6817 (1989).

⁷A. Amato, M. J. Graf, A. de Visser, H. Amitsuka, D. Andreica, and A. Schenck, *J. Phys.: Condens. Matter* **16**, S4403 (2004).

⁸K. Matsuda, Y. Kohori, T. Kohara, K. Kuwahara, and H. Amitsuka, *Phys. Rev. Lett.* **87**, 087203 (2001).

⁹O. O. Bernal, C. Rodrigues, A. Martinez, H. G. Lukefahr, D. E. MacLaughlin, A. A. Menovsky, and J. A. Mydosh, *Phys. Rev. Lett.* **87**, 196402 (2001).

¹⁰S. Saitoh, S. Takagi, M. Yokoyama, and H. Amitsuka, *J. Phys. Soc. Jpn.* **74**, 2209 (2005).

¹¹A. F. Santander-Syro, M. Klein, F. L. Boariu, A. Nuber, P. Lejay, and F. Reinert, *Nat. Phys.* **5**, 637 (2009).

¹²I. Kawasaki, S. I. Fujimori, Y. Takeda, T. Okane, A. Yasui, Y. Saitoh, H. Yamagami, Y. Haga, E. Yamamoto, and Y. Ōnuki, *Phys. Rev. B* **83**, 235121 (2011).

¹³A. R. Schmidt, M. H. Hamidian, P. Wahl, F. Meier, A. V. Balatsky, J. D. Garrett, T. J. Williams, G. M. Luke, and J. C. Davis, *Nature (London)* **465**, 570 (2010).

¹⁴C. Broholm, J. K. Kjems, W. J. L. Buyers, P. Matthews, T. T. M. Palstra, A. A. Menovsky, and J. A. Mydosh, *Phys. Rev. Lett.* **58**, 1467 (1987).

¹⁵A. Villaume, F. Bourdarot, E. Hassinger, S. Raymond, V. Taufour, D. Aoki, and J. Flouquet, *Phys. Rev. B* **78**, 012504 (2008).

¹⁶T. Nagao and J. I. Igarashi, *J. Phys. Soc. Jpn.* **74**, 765 (2005).

¹⁷H. C. Walker, R. Caciuffo, D. Aoki, F. Bourdarot, G. H. Lander, and J. Flouquet, *Phys. Rev. B* **83**, 193102 (2011).

¹⁸H. Amitsuka, M. Sato, N. Metoki, M. Yokoyama, K. Kuwahara, T. Sakakibara, H. Morimoto, S. Kawarazaki, Y. Miyako, and J. A. Mydosh, *Phys. Rev. Lett.* **83**, 5114 (1999).

¹⁹E. Hassinger, G. Knebel, K. Izawa, P. Lejay, B. Salce, and J. Flouquet, *Phys. Rev. B* **77**, 115117 (2008).

²⁰M. Yokoyama, H. Amitsuka, K. Tenya, K. Watanabe, S. Kawarazaki, H. Yoshizawa, and J. A. Mydosh, *Phys. Rev. B* **72**, 214419 (2005).

²¹Y. S. Oh, K. H. Kim, P. A. Sharma, N. Harrison, H. Amitsuka, and J. A. Mydosh, *Phys. Rev. Lett.* **98**, 016401 (2007).

²²M. Nakashima, H. Ohkuni, Y. Inada, R. Settai, Y. Haga, E. Yamamoto, and Y. Onuki, *J. Phys.: Condens. Matter* **15**, S2011 (2003).

- ²³E. Hassinger, G. Knebel, T. D. Matsuda, D. Aoki, V. Taufour, and J. Flouquet, *Phys. Rev. Lett.* **105**, 216409 (2010).
- ²⁴R. Okazaki, T. Shibauchi, H. J. Shi, Y. Haga, T. D. Matsuda, E. Yamamoto, Y. Onuki, H. Ikeda, and Y. Matsuda, *Science* **331**, 439 (2011).
- ²⁵N. Kernavanois, P. D. de Rotier, A. Yaouanc, J. P. Sanchez, K. D. Li, and P. Lejay, *Physica B: Condens. Matter* **259–261**, 648 (1999).
- ²⁶K. Kuwahara, H. Amitsuka, T. Sakakibara, O. Suzuki, S. Nakamura, T. Goto, M. Mihalik, A. A. Menovsky, A. de Visser, and J. J. M. Franse, *J. Phys. Soc. Jpn.* **66**, 3251 (1997).
- ²⁷J. A. Mydosh and P. M. Oppeneer, *Rev. Mod. Phys.* **83**, 1301 (2011).
- ²⁸S. Fujimoto, *Phys. Rev. Lett.* **106**, 196407 (2011).
- ²⁹P. M. Oppeneer, J. Ruzs, S. Elgazzar, M.-T. Suzuki, T. Durakiewicz, and J. A. Mydosh, *Phys. Rev. B* **82**, 205103 (2010).
- ³⁰P. M. Oppeneer, S. Elgazzar, J. Ruzs, Q. Feng, T. Durakiewicz, and J. A. Mydosh, *Phys. Rev. B* **84**, 241102 (2011).
- ³¹T. Das, [arXiv:1201.2246](https://arxiv.org/abs/1201.2246).
- ³²P. Chandra, P. Coleman, and R. Flint (unpublished).
- ³³In free space these order parameters are composed mainly of rank-5 operators mixed with rank-3 operators.
- ³⁴P. Thalmeier and T. Takimoto, *Phys. Rev. B* **83**, 165110 (2011).
- ³⁵This representation transforms as $\sim(xz, yz)$.
- ³⁶Note that this mechanism does not work for the other E -type order parameter, as there is no other E -type order parameter with the required quadrupole moments within the Γ_7 doublets.
- ³⁷A similar superspin relation between the HO and AF was suggested in Ref. 39 where the HO is hexadecapolar and related to the AF through a U(1) transformation. This hexadecapolar order parameter does not break tetragonal symmetry and is thus inconsistent with the torque experiment.
- ³⁸H. Ikeda, M. Suzuki, R. Arita, T. Takimoto, T. Shibauchi, and Y. Matsuda, *Nat. Phys. Lett.*, doi: [10.1038/nphys2330](https://doi.org/10.1038/nphys2330) (2012).
- ³⁹K. Haule and G. Kotliar, *Europhys. Lett.* **89**, 57006 (2010).